



PULSAR TIMING SOLUTIONS FOR 17 PULSARS AT 150 MHz FROM THE IRISH LOFAR STATION

D. J. MCKENNA 

ASTRON, The Netherlands Institute for Radio Astronomy, Oude Hoogeveensedijk 4, 7991 PD Dwingeloo, The Netherlands

E. F. KEANE 

School of Physics, Trinity College Dublin, College Green, Dublin 2, D02 PN40, Ireland.

P. T. GALLAGHER 

Astronomy & Astrophysics Section, School of Cosmic Physics, Dublin Institute for Advanced Studies, DIAS Dunsink Observatory, Dublin D15 XR2R, Ireland

J. MCCAULEY 

School of Physics, Trinity College Dublin, College Green, Dublin 2, D02 PN40, Ireland.

Version May 25, 2026

Abstract

Pulsar timing is a foundational part of pulsar research to triage the most interesting systems and to characterise properties (rotational or otherwise) of the population of these extreme objects. Due to the efficiency of a number of sensitive and/or wide-field surveys in recent years, the number of new pulsars discoveries is growing year-on-year, and most of these lack even basic timing parameter measurements. This work aims to demonstrate the capabilities of international Low Frequency Array (LOFAR) stations operating as single telescopes to follow-up, time and characterise these sources, offering new insight into the emission properties of these neutron stars, and support efforts to build timing models for these sources. Between 2020 and 2023 we used the local-mode allocation of the Irish LOFAR station to follow-up 33 pulsar candidates announced from various surveys at different observing frequencies to determine if an international LOFAR station has sufficient sensitivity to detect and time these sources. From the 33 pulsars selected, 22 pulsars were detected and 17 were selected for long-term monitoring across 590 h of observing time. This has resulted in coherent timing solutions for all of these sources at 150 MHz — 7 of these have never had any reported timing solutions, the remaining 10 solutions agree well with announcements from others since the beginning of our project. For a fraction of sources announced by surveys each year, the 14 international LOFAR stations are well placed to follow-up survey candidates for long-term pulsar monitoring beyond the standard timing campaigns performed at these telescopes to date, reducing the pressure on observing time availability at these observatories, and enabling the full scientific potential of these pulsars to be realised.

Subject headings: methods: observational, astronomical databases: miscellaneous, ephemerides, (stars:) pulsars: general

1. INTRODUCTION

Pulsar timing is essential for characterising the rotational behaviour of pulsars, and is a foundational step in enabling a plethora of scientific applications (Lorimer and Kramer 2005; Verbiest *et al.* 2021). Without timing it is almost impossible to identify the most interesting systems or to understand population properties. However regular monitoring of hundreds to thousands of pulsars, additionally ensuring broad frequency coverage, is intractable for most observatories given the over-subscription rates for the scarcest resource — observing time.

International LOFAR stations are commonly used to perform pulsar observations during local mode opera-

tions. They are well-equipped for the task, with large fractional bandwidths and reasonably good gain at their frequencies (van Haarlem *et al.* 2013). The available observing time is also considerable, especially as there are currently 14 such stations which make up the extended baselines of the International Low Frequency Array Telescope (ILT).

Several international Low Frequency Array (LOFAR) stations utilise a significant amount of their weekly time allocation to observe and monitor a wide range of pulsars. Recent works demonstrating these efforts range from follow-up of *Fermi* gamma-ray pulsars (Grießmeier *et al.* 2021), monitoring dispersion measure variations to detect free-electron variability associated with the interstellar medium and solar wind (Donner *et al.* 2020; Susarla *et al.* 2024), and the characterisation of the sub-

100 MHz population of pulsars (Bondonneau *et al.* 2020).

Over the past decade a large number of pulsars have been detected and have not received sufficient (or any) follow-up observations or timing analysis to determine their underlying rotation models. This means that any ephemerides for these sources can contain large uncertainties in the estimates for sky position, dispersion measure uncertainty and rotation period, often with no higher-order rotation terms quantified. At the beginning of this project (late 2020) the pulsar catalogue¹ (v1.64, Manchester *et al.* 2005) contained 452 sources that met this description.

Since then the pulsar discovery rates have increased so that this situation continues: v1.70 (v2.6.0) listed 743 (957) pulsars with no period derivative measured. These sources may not have been timed for many reasons, most likely from a lack of available observing time.

The Five-Hundred-Metre Aperture Spherical Telescope (FAST), operating at L band, is responsible for most recent discoveries (Han *et al.* 2021; Zhou *et al.* 2023; Han *et al.* 2025) meaning other telescopes, even 100-m class telescopes, cannot feasibly time these pulsars at L band as significantly more observing time per source is needed both for timing *and* to overcome the gain disparity. However as pulsar spectra are often quite steep (Jankowski *et al.* 2018) a possible avenue for progress is to time these sources at lower frequency.

In this paper we describe our efforts to detect and monitor a fraction of this population of pulsars that were without timing-derived ephemerides at the start of this project; our observations used the Irish LOFAR station. We begin by describing the criteria for our source selection in § 2 and the processing methodology in § 3. We then present an overview of the source properties we measured in this project, and discuss the implications of this work in § 4, before concluding in § 5.

2. SOURCE SELECTION

Even before the recent influx of pulsar discoveries it was clear that LOFAR had potential for pulsar timing. LOFAR Tied-Array All-Sky Survey (LOTAAS) reported nearly 400 pulsars, detectable with LOFAR (Sanidas *et al.* 2019), many of which were not observed on a regular basis.

The sources selected for this work were initially derived from the catalogues used for a rotating radio transient (RRAT, McLaughlin *et al.* 2006) census at I-LOFAR described in McKenna *et al.* (2024a), but was later expanded to use normal pulsars reported by various catalogues produced during the same surveys, or using the same telescopes, in June 2021. The sources observed consisted of those within the LOTAAS survey without reported parameters, from the Pushchino Radio Astronomy Observatory catalogues (PRAO, blind searches and PUMPs; 111 MHz; Tyul’bashev *et al.* 2016; Tyul’bashev *et al.* 2024), Green Bank North Celestial Cap survey (GBNCC; 350 MHz; Stovall *et al.* 2014), Arecibo Pulsar Survey using the Arecibo L-band Feed Array (Cordes *et al.* 2006, PALFA; 1420 MHz) and Arecibo 327 MHz drift scan survey (AO327; Deneva *et al.* 2013). We note some of these sources were later re-detected during the Targeted search, Using LoTSS Im-

ages, for Polarised Pulsars project (TULIPP; overlapping bandwidth with this work; Sobey *et al.* 2022) and FAST Galactic Plane Pulsar Snapshot survey (FAST GPPS; 1250 MHz; Han *et al.* 2021).

Reported source pointings, periods, and dispersion measures were cross-referenced between the sampled catalogues to ensure a lack of duplicated sources. Many surveys provide initial estimates for source parameters on their websites, but we found that candidate plots, produced by programs such as `prepfold` (Ransom 2011), also provided alongside such tables often provided more significant figures for the source parameters, even after accounting for instrumental uncertainty and source evolution over time. A number of initial positions, rotation periods and dispersion measures were thus manually extracted from these candidate plots.

This resulted in 33 (see Table 4) sources being selected as they had wide uncertainties on their existing basic ephemeris parameters and lacked published timing solutions for observations with I-LOFAR. Initially, this consisted of observations to determine if they could be detected, and if so, to monitor these for characterisation by performing pulsar timing on a long-term basis.

3. METHODOLOGY

3.1. Observations

Observations for sources to monitor as a part of this work that had not been observed as a part of the RRAT census discussed in McKenna *et al.* (2024a) began in June 2021 and continued until August 2022. Observations of sources were initially 59 min centered on the transit time of the source, although in the sources where weak emission was identified (as opposed to a non-detection), follow-up observations were extended to 89 min, nominally reducing the noise floor by 18%, to see if the observation criteria were met (see §3.2), before keeping or removing this source from the potential observing pool for longer term monitoring. The maximum observing window of 89 min was chosen, as longer observations on a regular basis with the station were deemed to be an excessive use of the 31 h of weekly observing time typically available for standalone operations at the time. Timing observations proceeded for these sources, however updated sky positions from pulsar timing were not utilised for observations until after this work (July 2023).

This was to ensure a consistent source pointing for the observations during follow-up observations to simplify later (spectral-) flux density analysis, as opposed to continuously deployed incrementally better sky positions over time. Dispersion measures were updated for coherent dedispersion as soon as deviations between the candidate ephemerides and detected emission were noted.

Observations were pre-processed using the standard I-LOFAR observing system, and RRAT processing pipeline (McKenna *et al.* 2024a). Observations were taken with the LOFAR HBA tiles in band ‘110_190’, with subbands 12 to 499 beam-formed on the best-known position of the sources. This covers 102.2–197.56 MHz, for a total bandwidth of 95.51 MHz. Typically, 5% of the band edges are unusable due to the high- and low-pass filters at 100 and 200 MHz, and additional FM-band radio emissions near 100 MHz. The analysed data are further restricted, as described below in §3.3.

¹ <https://www.atnf.csiro.au/research/pulsar/psrcat/>

Data are recorded to disk and processed using a modified version of `CDMT`² (Bassa *et al.* 2017), using `UDP-PACKETMANAGER` (McKenna *et al.* 2024b) to prepare voltages instead of reading Central Processing (CEP)-produced `HDF5` files. `cdmt_udp` is used to perform channelisation, coherent dedispersion and filterbanking of raw voltages on the Nvidia Tesla V100s in the local compute cluster (Murphy *et al.* 2021). The data were processed in a common manner across all observations, with a channelisation factor of 8, producing 24.41 kHz channels, and temporal down-sampling at a factor of 16, producing 655.36 μ s samples. Each datum is stored as a 32-bit floating point value by default, before being re-sampled using the `digifil` tool, which is part of the `DSPSR` software suite (van Straten and Bailes 2011), to re-sample the data as 8-bit samples, using the default 10s re-scaling interval.

The 32-bit floating point filterbank for each observation is compressed using `ZSTANDARD` (Collet and Kuchera 2018) and archived by default. In the case that a source is not detected after 6 months, the archived filterbank may undergo spectral downsampling by a factor of 8, using `digifil` without interval re-scaling, to reduce the on-disk size of the archived filterbank, and return it to the original spectral resolution of the data.

3.2. Detection and Timing Criteria

The data were initially processed with `PRESTO`'s `prepfold` tool to search for indications of emission after each observation. Two searches were performed per observation, one narrow search focusing on a fixed-Dispersion Measure (DM) trial width³, while further searches were manually performed with numerous period trials, and a narrow DM search window⁴. A source was deemed to be sufficiently bright to be timed if it could produce a Signal-to-Noise Ratio (S/N) of 6 or greater within the detected observing window, after generating a folded archive with `dspsr` and then performing S/N optimisation with `pdmp` (Hotan *et al.* 2004). An alternative criterion was applied to nulling or intermittent sources in the case that emission *windows* provided sufficient S/N to be independently selected and timed when off-modes were zapped from the initial observation. Following this, sources were investigated to determine if there were ongoing (or completed) efforts to time the source by investigators associated with the surveys by using public observation databases, such as the LOFAR Long Term Archive (LTA). In the case that the sources were not a part of observing campaigns elsewhere, follow-up observations were scheduled for the weeks post-detection to begin timing the sources at The Irish Low Frequency Array Station (I-LOFAR).

3.3. Data Processing and Analysis

The 8-bit filterbank of observations were initially folded using trial parameters derived from the survey candidate announcement and best-fit `prepfold` parameters in an ephemeris using `dspsr`. Archives were formed

with 256 bins per frequency channel across 30-second integrations. `clfd` (Morello *et al.* 2019) was then used to remove Radio Frequency Interference (RFI) from each archive. Time of Arrivals (TOAs) were generated using `PSRCHIVE` (Hotan *et al.* 2004), whereby the longest observation was used to generate a analytic template model with `paas` to determine TOA measurements for each observation with `pat`, for initial timing efforts. During this early stage, it was found that the parabolic interpolation shift (PIS) method that was typically used for generating single pulse TOA was not performing as expected for the observed periodic emission. The measurement uncertainties, especially for weaker sources, appeared to be severely underestimated by the algorithm⁵. As a result, for the data described here, the Fourier-Domain Markov Chain Monte-Carlo (FDM) method was used to produce TOA measurements, following a comparison of the uncertainties associated with available options. Timing and ephemeris production was performed using `TEMPO2` (Hobbs *et al.* 2006).

When timing a pulsar from scratch it is necessary to perform an iterative process to finalise solutions. Once timing solutions were obtained for all sources, in July 2023, each observation was re-folded with 1024 bins per frequency channel with 10-second integrations to improve the archive quality and offer the opportunity to investigate the nulling behaviour of some sources across shorter durations. Additionally, in the case that a source had undergone spectral down-sampling after a non-detection, each full-resolution filterbank was re-processed to achieve a common spectral resolution. The archives were not down-sampled as it was found that the `fscrunch` function did not appear to re-normalise the channel data when archives were re-sampled, causing archives generated from spectrally down-sampled filterbanks to have weak contributions in S/N calculations. After a coherent timing solution was found, final 1-dimensional analytic timing templates were formed using the full set of observations combined with `psradd` using `paas`, and sources were re-fit using the final TOAs measurements.

Source spectral flux density calculations were performed on the full corpus of observations for each source, in 10-MHz bandwidth blocks centred on frequencies in decreasing steps from 181–121 MHz. Given the known off-sets of each source inside the LOFAR stations beam, a corrected value is produced considering the offset from a Gaussian beam of known Full Width at Half Maximum (FWHM) (including the 1.02 correction factor, see Table B.1 of van Haarlem *et al.* (2013) for details), for the spectral flux densities. Flux densities are derived from the modified radiometer equation in Equation 1, which for LOFAR is typically derived from the work of Kondratiev *et al.* (2016). The specific modifications made for this work were previously discussed in McKenna *et al.* (2024a), which gives:

$$S(\nu, l, b) = S/N \frac{2k_B (T_{\text{sky}}(\nu, l, b) + T_{\text{ant}})}{A_{\text{eff}}(\nu) m_{\Pi}(\nu, l, b, t) \beta \gamma} \Delta, \quad (1)$$

$$\Delta = \frac{1}{\sqrt{n_p \Delta \nu_{\text{eff}} t_{\text{obs}}}} \sqrt{\frac{W}{P - W}},$$

⁵ A pointing of a non-detected intermittent source had an uncertainty below 20 μ s, less than 5% of the width of a single time sample of the input, and below 10% of the bin width

² <https://github.com/David-McKenna/cdmt>

³ Using flags `-nodmsearch -nopdsearch -fine`

⁴ `-npfact` was varied from 2–8, while `-ndmfact -dmstep` were kept at 3 and 1

where l and b are Galactic coordinates. Several factors like k_B the Boltzmann constant, $n_p = 2$ the number of polarisations, the processing correction factor β accounting for the 8-bit digitisation losses (below 1%) and S/N losses due to using a boxcar as a reference (Morello *et al.* 2019, about 6%), are constant between all calculations. For a frequency, ν , we sample the sky temperature, T_{sky} , using a primary-beam-lobe-convolved copy of the Low Frequency Sky Model (LFSM, Dowell *et al.* 2017), as provided by PYGDSM (Price 2021) and both the antenna temperature, T_{ant} and effective collecting area at zenith, A_{eff} , for the LOFAR system (Wijnholds and van Cappellen 2011). A Mueller matrix is derived from a Jones matrix calculated by DREAMBEAM (Carozzi 2020) to correct for pointing losses with the factor m_{II} as a function of both frequency and altitude and azimuth, averaged across the galactic coordinates for the observing window of the observation. A source pointing error correction, γ , is calculated using a 2-dimensional Gaussian to correct for errors between the initial candidate and final timed location.

The post-RFI cleaning bandwidth ($\Delta\nu_{\text{eff}}$), is extracted from the CLFD report files, while the pulse width (W), dispersion measure and S/N are calculated using `pdmp.vap` is used to determine the total integrated time in the final output archive. The spectral behaviour of the data described above was fit using power laws and least-squared modelling in PYTHON using the LMFIT package (Newville *et al.* 2021). The above procedures combined result in a measurement of the source flux density with an absolute scale uncertainty of 50% (Bilous *et al.* 2016; Kondratiev *et al.* 2016).

4. RESULTS AND DISCUSSION

From observations of 33 sources, 17 were chosen to be monitored out of 22 sources with detectable emission (full list of observations available in Tables 4 and 5). Over 400 h of telescope time were used to time these sources between December 2020 and July 2023. The overall source properties can be found in Table 1. These sources were announced as pulsar candidates between 2012 and 2020, cover a rotation period range of 0.04–3.53 s with pointing-corrected flux densities at 150 MHz ranging from 1.6–90.8 mJy. Duty cycles ranged from 1.0% to 13.8%.

While there was insufficient sensitivity to perform a nulling analysis, a number of sources were observed to have variability in their waterfall plots when heavily downsampled, and are noted in Table 1 with a dagger † suffix. Sources that appeared to have some nulling characteristics include PSRs J0104+6438, J0220+3626, J0317+1328 and J2105+1908. This was expected for PSRs J0317+1328 and J2105+1908 as these were previously reported as RRATs by Tyul’bashev *et al.* (2018). PSRs J1327+3423, J1536+1759 and J2202+2134 were observed to have high flux density variability between observations, but were reasonably stable within single observing windows; PSR J1536+1759 is discussed further in § 4.2.4.

DM_PHASE (Seymour *et al.* 2019) was investigated as an alternative method to calculate dispersion measures, however it was found to provide at least one order of magnitude higher uncertainties for smooth, single component pulse profiles, which make up the majority of the

sources in this work (see Fig. 2). Given it was originally authored with the goal of optimising complex fast radio burst pulses from the CHIME telescope (CHIME/FRB Collaboration *et al.* 2019), this is not a completely unexpected result.

Pulsar timing was performed for all sources, and coherent solutions were found in all cases. Ephemerides for each of the sources can be found in Tables 3 and 2. Source positions are reported with uncertainties at arc-second level or better. While estimates have been provided for the source distances based on the Ocker and Cordes (2026) NE2025 model, one source (PSR J1243+3946) has only a lower limit distance estimate as it exceeds the maximum expected dispersion measure for its line of sight within the Milky Way. The average summed profiles after dedispersion and RFI flagging are provided in Figure 2.

In this work a population analysis was not conducted given these sources represent a filtered selection of sources from multiple telescopes, observed at multiple frequencies, each of which have their own selection criteria for detecting new pulsars, which were then further filtered by the selection criteria of the LOFAR telescope.

4.1. Previously Timed Sources

From these 17 sources, 10 had timing solutions produced at the time of submission of this work. This includes the CHIME PSR J0226+3356 (Dong *et al.* 2023), LOTAAS PSR J0317+1328 (Wateren *et al.* 2023), GBT PSR J1327+3423 (Fiore *et al.* 2023), PALFA PSRs J0608+1635 and J2000+2920 (Parent *et al.* 2022) and AO327 PSRs J1832+2749 and J2347+0300 (Olszanski *et al.* 2025). Three further sources, PSRs J0104+6438, J0355+2838 and J1837+5156, appear in the GBNCC GitHub Data repository⁶ and cite the work of McEwen *et al.* (2024).

The ephemerides produced as a part of this work fall within the expectations of the models produced by the cited works. Primarily due to the frequency range of LOFAR, our determined dispersion measure uncertainties are reduced over previous works for the monitored sources, or overlap the uncertainties provided (PSRs J1327+3423, J1832+2749, J2347+0300).

4.2. Sources of note

4.2.1. PSR J0220+3626

PSR J0220+3626 has previously been reported to be a pulsar with sub-pulse drifting and giant pulses by the PRAO (Teplykh *et al.* 2022). While I-LOFAR lacks the sensitivity to probe the sub-pulse properties of the source, 9 single pulses were detected from the source as a part of this work. Our measurement of a FWHM of 141 ms at 150 MHz is consistent with the findings of Teplykh *et al.* (2022) who found a ~ 220 ms main pulse component at 111 MHz.

4.2.2. PSR J0355+2838

In the work of McEwen *et al.* (2020), PSR J0355+2838 was reported with a significantly modified period that is present in the current version of the pulsar catalogue

⁶ <https://github.com/GBNCC/data>

Source	Cat.	Year	Period (s)	DM (pc cm ⁻³)	T _{obs} (h)	w ₅₀ (ms)	D.C. %	Measured		Corrected		
								S ₁₅₀ (mJy)	α	θ _{off} (deg)	S ₁₅₀ (mJy)	α
J0104+6438†	GL	2012	1.3862	42.026(9)	20.4	37(7)	2.7	5.8	-0.9(2)	0.10	5.8	-0.9(2)
J0146+3055	P	2016	0.9381	25.791(6)	24.6	26(5)	2.8	7.2	-3.1(3)	0.34	7.6	-3.0(3)
J0220+3626†	GL	2016	1.0298	45.45(3)	19.1	141(12)	13.8	13.9	-1.63(12)	0.00	13.9	-1.63(12)
J0226+3356	C	2020	1.2401	27.386(10)	26.0	50(8)	4.1	3.4	-0.4(3)	0.05	3.4	-0.4(3)
J0317+1328†	LP	2014	1.9742	12.779(12)	12.6	23(7)	1.2	4.2	-1.4(3)	0.28	4.4	-1.4(3)
J0355+2838	GL	2014	0.3649	48.734(6)	28.6	30(3)	8.5	6.9	-1.5(4)	0.18	7.0	-1.5(4)
J0608+1635	AL	2013	0.9458	86.146(6)	18.3	47(7)	5.0	23.7	-2.9(3)	0.21	24.2	-2.8(3)
J1132+2513	LP	2015	1.0021	23.716(6)	23.7	21(5)	2.1	9.3	-2.3(3)	0.30	9.7	-2.2(3)
J1243+3946	LP	2016	1.3103	26.462(8)	19.8	35(7)	2.7	7.9	-1.13(17)	0.24	8.1	-1.08(18)
J1327+3423†	GLP	2014	0.0415	4.1850(3)	6.1	2.4(7)	5.7	76.2	-2.9(3)	0.63	90.8	-2.5(3)
J1536+1759†	P	2017	0.9331	28.594(7)	47.7	19(4)	2.1	1.6	-2.8(4)	0.19	1.6	-2.8(4)
J1832+2749	AL	2014	0.6317	47.387(5)	34.2	31(4)	5.0	6.6	-0.80(12)	0.07	6.6	-0.79(12)
J1837+5156	GL	2014	0.6919	43.819(6)	32.9	48(6)	7.0	8.1	0.0(4)	0.22	8.3	0.0(4)
J2000+2920	AL	2015	3.0738	132.151(19)	38.4	102(18)	3.3	3.7	0.8(4)	0.18	3.7	0.8(4)
J2105+1908†	P	2018	3.5298	34.45(2)	17.6	84(17)	2.4	2.7	-2.6(5)	0.03	2.7	-2.6(5)
J2202+2134†	P	2020	1.3583	17.742(8)	28.5	13(4)	1.0	5.6	-1.89(18)	0.21	5.7	-1.85(18)
J2347+0300	AL	2016	1.3861	16.124(9)	18.1	25(6)	1.9	13.5	-2.4(6)	0.15	13.6	-2.4(6)

TABLE 1

THE OBSERVED PROPERTIES OF THE SOURCES CHOSEN FOR MONITORING AS A PART OF THIS WORK. THE TABLE CONTAINS COLUMNS FOR THE ORIGINAL SOURCE CATALOGS, THE YEAR OF DISCOVERY, A ROUNDED ROTATION PERIOD, THEIR DISPERSION MEASURE (DM), THE TOTAL OBSERVATION TIME (T_{obs}), THE FULL WIDTH AT HALF MAXIMUM (FWHM) OF EMISSION (w₅₀), THE DUTY CYCLE (D.C.), AND BOTH CORRECTED AND UNCORRECTED FLUX DENSITY AT 150 MHz AND SPECTRAL POWER LAW EXPONENT FOR THE EMISSION, CORRECTING FOR OFF-AXIS OBSERVATIONS WITH RESPECT TO THE FINAL TIMING LOCATION (θ_{off}). SOURCES WITH A DAGGER SUFFIX HAVE SHOWN SIGNS OF NULLING OR HIGHLY VARIABLE EMISSION. IN THE CATALOGUES COLUMN, WE NOTE SURVEYS WHERE PARAMETERS WERE REPORTED FOR THESE SOURCES DURING THE OBSERVING CAMPAIGN. “A” FOR WORK FROM THE ARECIBO TELESCOPE, “G” FOR THE GBNCC SURVEY, “L” FOR THE LOTAAS SURVEY, AND “P” IS THE PRAO CATALOGUES.

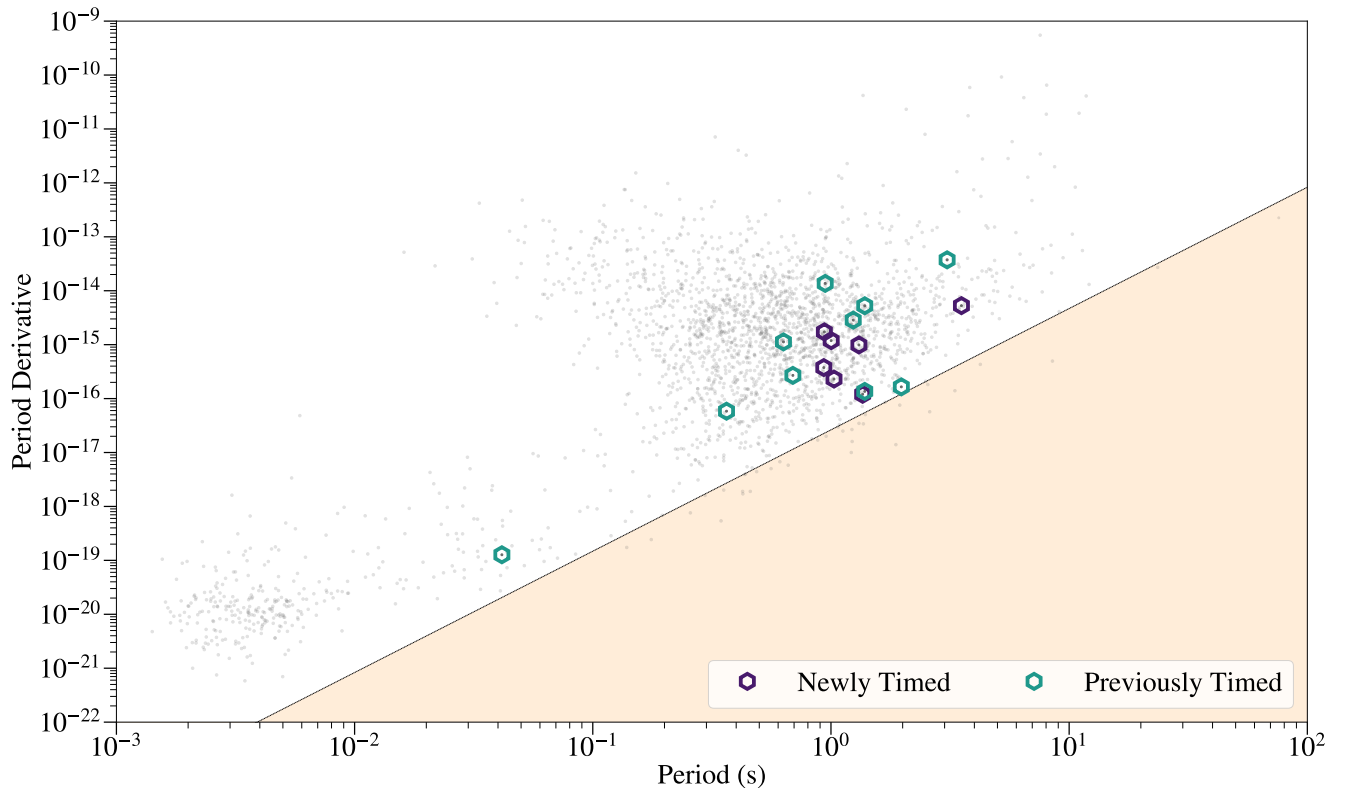


FIG. 1.— A period-period derivative phase space plot of known pulsars, with the sources timed as a part of this work highlighted. This plot was generated with the aid of PSRQPY (Pitkin 2018).

(v2.6.0), 94.3 ms, as opposed to the original survey period, the latter of which was used for this work and is present in the ephemeris, 364.9 ms. This does not appear to be an integer multiple of the final rotation period, and

we are uncertain how it was obtained. Periodic emission could not be detected from the source from the 4 longest observations of the source (each 89 min) at I-LOFAR, when the data were folded at trials for a topocentric pe-

Source	J0146+3055	J0220+3626	J1132+2513	J1243+3946
Survey	PRAO, FAST GPPS	GBNCC, PRAO, LOTAAS, TULIPP	GBNCC, PRAO, AR327, FAST GPPS	PRAO, FAST GPPS
Right Ascension (hms)	01 ^h 46 ^m 41 ^s 029(13)	02 ^h 20 ^m 42 ^s 16(12)	11 ^h 32 ^m 29 ^s 947(12)	12 ^h 43 ^m 03 ^s 509(10)
Declination (dms)	30°55'19''1(4)	36°26'55''(2)	25°13'32''6(4)	39°46'09''17(13)
Galactic Longitude (°)	136°67773(5)	142°3172(5)	214°61428(5)	130°24022(4)
Galactic Latitude (°)	-30°470883(98)	-23°0404(6)	72°20598(11)	77°23989(4)
Dispersion Measure (pc cm ⁻³)	25.791(6)	45.45(3)	23.716(6)	26.462(8)
Distance (pc)	1793	3244	5216	>8300
Period (s)	0.938062139694(16)	1.029795190912(97)	1.002131964901(10)	1.310291834197(14)
Period Derivative (10 ⁻¹⁵ s s ⁻¹)	1.7250(17)	0.23(3)	1.18842(97)	0.9873(18)
Characteristic Age (Myr)	8.62	71.7	13.4	21.0
Magnetic Field (10 ¹² G)	1.29	0.490	1.10	1.15
Timing Start (MJD)	59528	59528	59206	59521
Timing End (MJD)	60123	60010	60094	60107
Reference Epoch (MJD)	59857	59750	59750	59750
N _{TOAs}	20	19	33	21
RMS Residuals (μs)	705	4659	692	520

Source	J1536+1759	J2105+1908	J2202+2134
Survey	PRAO	PRAO	PRAO, GBNCC
Right Ascension (hms)	15 ^h 36 ^m 34 ^s 32(3)	21 ^h 05 ^m 30 ^s 61(8)	22 ^h 02 ^m 16 ^s 984(17)
Declination (dms)	17°59'24''7(7)	19°08'34''8(1.1)	21°34'33''6(4)
Galactic Longitude (°)	28°28365(12)	66°8555(3)	78°62145(7)
Galactic Latitude (°)	50°97946(19)	-18°3455(3)	-26°39566(12)
Dispersion Measure (pc cm ⁻³)	28.594(7)	34.48(2)	17.742(8)
Distance (pc)	4266	2622	1407
Period (s)	0.93312798225(9)	3.5298270014(3)	1.35830601223(2)
Period Derivative (10 ⁻¹⁵ s s ⁻¹)	0.376(9)	5.29(4)	0.1202(15)
Characteristic Age (Myr)	39.4	10.6	179
Magnetic Field (10 ¹² G)	0.599	4.37	0.409
Timing Start (MJD)	59626	59569	59226
Timing End (MJD)	60101	60108	60108
Reference Epoch (MJD)	59750	59850	59819
N _{TOAs}	27	14	16
RMS Residuals (μs)	1915	2521	518

TABLE 2

NOVEL TIMING EPHEMERIDES PRODUCED AT I-LOFAR AS A PART OF THIS WORK. THE DISTANCE MEASUREMENT OF PSR J1243+3946 INDICATES THAT IT EXCEEDS THE MAXIMUM DISPERSION MEASURE EXPECTED ALONG THE LINE OF SIGHT WITHIN THE MILKY WAY FROM THE NE2025 MODEL.

riod of 94.30(13) ms. While the pulsar is still represented with this shorter period in v2.6.0 of PSRCAT, given that the [GBNCC/data](#) GitHub repo (containing work from [McEwen et al. \(2024\)](#)) contains a new ephemeris matching the period we use here, this seems to be an error that will be corrected in a future release of the pulsar catalogue.

4.2.3. PSR J1327+3423

PSR J1327+3423 is a 41.5-ms rotation period pulsar with a low dispersion measure of 4.185 pc cm⁻³, with an ephemeris previously reported by [Fiore et al. \(2023\)](#), and also announced in the PRAO pulsar and RRAT catalogues. It is suspected to be a recycled pulsar given the timing solution determined it has a rotation derivative of 1.27×10^{-19} s s⁻¹. It was the fastest rotating source observed as a part of this work, and was initially not going to be monitored due to the relatively low number of time samples per rotation (63) produced with the standard pipeline and strong scattering at low frequencies.

However, it was noticed that due to its brightness it was visible as an off-axis source when observing RRAT J1336+3416 as a part of the work described

in [McKenna et al. \(2024a\)](#), which received a large amount of observing time due to the presence of a secondary off-axis pulse train in the single-pulse timing results. As a result, a sufficient number of TOAs could be generated for the source ‘for free’ using the J1336+3416 data, and we tried to form a coherent timing solution for the source given the data was available. These off-axis data were only used to determine TOAs for the source, e.g. not flux densities, and is not included in Table 1 or 4 for the source. The uncertainties on the TOAs measurements are relatively high despite the source brightness as a result of being observed off-axis, at a low number of samples per revolution, resulting in a model that can describe the overall basic parameters of the source, but cannot identify higher precision effects on the TOAs, such as the proper-motion parameters, reported by [Fiore et al. \(2023\)](#).

4.2.4. PSR J1536+1759

PSR J1536+1749 was observed to be extremely variable between observations during this work. It was only detected in preview `prepfold` plots for 55% of the observations (18 of 33, Table 4), with a mean observing time of

Source	J0104+6438	J0226+3356	J0317+1328	J0355+2838
Survey Solution	GBNCC GBNCC/data	CHIME Dong <i>et al.</i> (2023)	LOTAAS Wateren <i>et al.</i> (2023)	GBNCC GBNCC/data
Right Ascension (hms)	01 ^h 04 ^m 37 ^s .21(3)	02 ^h 26 ^m 57 ^s .14(3)	03 ^h 17 ^m 48 ^s .71(8)	03 ^h 55 ^m 22 ^s .89(4)
Declination (dms)	64°38′30″.0(2)	33°56′26″.7(7)	13°28′32″.4(4)	28°38′42″.2(2)
Galactic Longitude (°)	124°34340(14)	144°65706(13)	168°7491(3)	164°78042(16)
Galactic Latitude (°)	1°80604(7)	−24°8698(2)	−36°0598(10)	−18°9122(6)
Dispersion Measure (pc cm ^{−3})	42.026(9)	27.386(10)	12.779(12)	48.734(6)
Distance (pc)	2629	1803	747	2546
Period (s)	1.38618423347(3)	1.240102562457(15)	1.97423969309(5)	0.36492920980(3)
Period Derivative (10 ^{−15} s s ^{−1})	0.136(3)	2.8547(14)	0.165(4)	0.0584(15)
Characteristic Age (Myr)	162	6.89	190	99.0
Magnetic Field (10 ¹² G)	0.439	1.9	0.578	0.148
Timing Start (MJD)	59395	59177	59129	59401
Timing End (MJD)	60123	59982	59989	60031
Reference Epoch (MJD)	59759	59641	59500	59920
N _{TOAs}	37	16	17	32
RMS Residuals (μs)	1683	718	1409	2056
Source	J0608+1635	J1327+3423	J1832+2749	J1837+5156
Survey Solution	PALFA Parent <i>et al.</i> (2022)	GBNCC/PRAO Fiore <i>et al.</i> (2023)	AO327 Olszanski <i>et al.</i> (2025)	GBNCC GBNCC/data
Right Ascension (hms)	06 ^h 08 ^m 51 ^s .654(18)	13 ^h 27 ^m 07 ^s .547(3)	18 ^h 32 ^m 19 ^s .002(13)	18 ^h 37 ^m 51 ^s .25(2)
Declination (dms)	16°35′02″.3(3)	34°23′37″.66(5)	27°49′36″.2(2)	51°56′14″.6(2)
Galactic Longitude (°)	193°36751(8)	78°605524(12)	56°35782(5)	80°95498(10)
Galactic Latitude (°)	−1°5704(7)	79°446663(14)	16°16734(6)	23°04883(7)
Dispersion Measure (pc cm ^{−3})	86.146(6)	4.1850(3)	47.387(5)	43.819(6)
Distance (pc)	2107	532	3440	3633
Period (s)	0.94584729633(3)	0.04151271040323(15)	0.631706905364(9)	0.691906460248(12)
Period Derivative (10 ^{−15} s s ^{−1})	13.675(3)	0.000127(12)	1.1249(10)	0.2694(16)
Characteristic Age (Myr)	1.1	5180	8.9	40.7
Magnetic Field (10 ¹² G)	3.64	0.00232	0.853	0.437
Timing Start (MJD)	59395	59248	59382	59382
Timing End (MJD)	60052	60101	60108	60102
Reference Epoch (MJD)	59750	59750	59750	59750
N _{TOAs}	41	50	37	38
RMS Residuals (μs)	2287	218	1368	1717
Source	J2000+2920	J2347+0300		
Survey Solution	PALFA Parent <i>et al.</i> (2022)	AO327 Olszanski <i>et al.</i> (2025)		
Right Ascension (hms)	20 ^h 00 ^m 16 ^s .57(7)	23 ^h 47 ^m 44 ^s .41(4)		
Declination (dms)	29°20′07″.4(1.2)	03°00′14″.4(1.2)		
Galactic Longitude (°)	66°5494(3)	93°44425(15)		
Galactic Latitude (°)	−0°3527(3)	−56°1771(3)		
Dispersion Measure (pc cm ^{−3})	132.151(19)	16.124(9)		
Distance (pc)	6523	1154		
Period (s)	3.0737882818(2)	1.386056611589(9)		
Period Derivative (10 ^{−15} s s ^{−1})	37.40(3)	5.2657(12)		
Characteristic Age (Myr)	1.30	4.17		
Magnetic Field (10 ¹² G)	10.8	2.73		
Timing Start (MJD)	59381	59395		
Timing End (MJD)	60102	60108		
Reference Epoch (MJD)	59750	59750		
N _{TOAs}	32	21		
RMS Residuals (μs)	6064	495		

TABLE 3
TIMING SOLUTIONS FOR SOURCES THAT HAVE PREVIOUSLY BEEN ANNOUNCED BY WORK AT OTHER TELESCOPES.

1.45 h. Initially, TOAs were only generated for observations which had detectable emission in the preview plots, which were then used to form the initial timing model for the source. Afterwards, all TOAs were included in the fit, however only an additional 4 TOAs from the 15 non-

visual-detections were used for the timing solution as the remaining TOAs had large uncertainties, or large phase offsets. Notably, during an extended local mode window with the station, the source went undetected across 5 observations spread across 6 days. While the previous

59 min observation of the source had shown a S/N of 5.5, during this period it was not detected with observations of 89, 89, 119, 149 and 89 min in length. These observations indicate this source may be a nulling pulsar or an intermittent pulsar.

4.2.5. PSR J2105+1908

PSR J2105+1908 was observed following a detection and localisation during observations taken with the LOFAR core (McKenna et al., in prep., LOFAR project code LC16_016). At the time of that work, the source did not have a known period, and was not initially observed as a part of the I-LOFAR RRAT census (McKenna et al. 2024a) due to the low reported peak flux density by the PRAO. Follow-up observations after the core detection and localisation allowed for periodic emission to be detected from the source, however no single pulses were detected during the 17.6 h of observations performed prior to July 2023. Tyul’bashev et al. (2022) later reported a rotation period of 3.5297s which aligns with the result obtained during the LOFAR core work, and our final timing solution presented in Table 2.

The nulling behaviour of the source, previously observed as 0.38(11) with the LOFAR core, has not yet been characterised for our I-LOFAR observations, as initial attempts to separate the modes demonstrated that the active mode was too quiet to be detected in the typical 10–30s integration used for this analysis. While increasing the integration time further may allow for the two modes to be separated, the short switching duration observed from the LOFAR core observation, and small N statistics means this is not likely to result in an accurate value, or reduce the uncertainty from the LOFAR core observation.

5. CONCLUSIONS

We have presented 17 pulsar timing ephemerides for pulsars generated from observations using I-LOFAR at 150 MHz between 2020 and 2023. From these, 7 sources did not have previous ephemerides published, while the remaining 10 match recently announced results from other telescopes. Systemic analysis was performed to describe the emission properties of the sources, which were found to have flux densities at 150 MHz ranging from 2–91 mJy, with spectral indices from -3.0 to $+0.8$.

Duty cycles ranged from 1.0% to 14%. 5 of the observed sources showed signs of nulling or highly variable emission.

This work demonstrates the effectiveness of international LOFAR stations for establishing timing solutions for newly discovered pulsars. This has been shown to be feasible even for pulsars where very scant initial information is available, i.e. they can be timed completely ‘from scratch’, and even for pulsars discovered by instruments with much larger gain. The latter leverages the spectra of pulsars which are typically brighter at low frequencies.

As the discovery rate of pulsars is accelerating, thanks to FAST, and looks set to accelerate even more when the Square Kilometre Array telescopes (currently under construction) are operational during this decade, the need for other telescopes to time pulsars is ever growing. This timing procedure is essential for, at the very least, triaging discoveries to identify systems most suitable for dedicated deep monitoring, but also for properly characterising the spin evolution of the pulsar population at large. We will continue and expand upon the work presented here.

ACKNOWLEDGMENTS

D.J.McK acknowledges funding under the Government of Ireland Postgraduate Scholarship (GOIPG/2019/2798) administered by the Irish Research Council (IRC). D.J.McK and E.F.K. would like to thank Aaron Golden of the University of Galway for hosting them on numerous ‘busy weeks’ which helped immensely in getting this work to completion. The Rosse Observatory is operated by Trinity College Dublin. I-LOFAR infrastructure has benefited from funding from Science Foundation Ireland, a predecessor of Taighde Éireann — Research Ireland.

DATA AVAILABILITY

Folded profiles and times of arrival per-observation and averaged across the entire set of observations can be found on Zenodo (McKenna 2025a). Stokes I filterbanks or pre-time and frequency scrunched archives can be made available on a request to the contact author.

tempo2 pulsar timing solutions presented in Tables 2 and 3 can be found on Zenodo (McKenna 2025b) in a machine-readable format.

REFERENCES

- D. R. Lorimer and M. Kramer, *Handbook of Pulsar Astronomy*, Cambridge observing handbooks for research astronomers, Vol. 4 (Cambridge University Press, 2005).
- J. P. W. Verbiest, S. Osłowski, and S. Burke-Spolaor, in *Handbook of Gravitational Wave Astronomy*, edited by C. Bambi, S. Katsanevas, and K. D. Kokkotas (2021) p. 4.
- M. P. van Haarlem, M. W. Wise, A. W. Gunst, G. Heald, J. P. McKean, J. W. T. Hessels, A. G. de Bruyn, R. Nijboer, J. Swinbank, R. Fallows, M. Brentjens, A. Nelles, R. Beck, H. Falcke, and et al., *Astronomy & Astrophysics* **556**, A2 (2013).
- J.-M. Grießmeier, D. A. Smith, G. Theureau, T. J. Johnson, M. Kerr, L. Bondonneau, I. Cognard, and M. Serylak, *Astronomy & Astrophysics* **654**, A43 (2021).
- Donner, Verbiest, J. P. W., Tiburzi, C., Osłowski, S., Künsemöller, J., Bak Nielsen, A.-S., Grießmeier, J.-M., Serylak, M., Kramer, M., Anderson, J. M., Wucknitz, O., Keane, E., Kondratiev, V., Sobey, C., McKee, J. W., Bilous, A. V., Breton, R. P., Brüggem, M., Ciardi, B., Høft, M., van Leeuwen, J., and Vocks, C., *A&A* **644**, A153 (2020).
- S. C. Susarla, A. Chalumeau, C. Tiburzi, E. F. Keane, J. P. W. Verbiest, J. S. Hazboun, M. A. Krishnakumar, F. Iraci, G. M. Shaifullah, A. Golden, A. S. Bak Nielsen, J. Donner, J. M. Grießmeier, M. J. Keith, S. Osłowski, N. K. Porayko, M. Serylak, J. M. Anderson, M. Brüggem, B. Ciardi, R. J. Dettmar, M. Høft, J. Künsemöller, D. Schwarz, and C. Vocks, *A&A* **692**, A18 (2024).
- L. Bondonneau, J. M. Grießmeier, G. Theureau, A. V. Bilous, V. I. Kondratiev, M. Serylak, M. J. Keith, and A. G. Lyne, *A&A* **635**, A76 (2020).
- R. N. Manchester, G. B. Hobbs, A. Teoh, and M. Hobbs, *The Astronomical Journal* **129**, 1993 (2005).
- J. L. Han, C. Wang, P. F. Wang, T. Wang, D. J. Zhou, J.-H. Sun, Y. Yan, W.-Q. Su, W.-C. Jing, X. Chen, X. Y. Gao, L.-G. Hou, J. Xu, K. J. Lee, N. Wang, P. Jiang, R.-X. Xu, J. Yan, H.-Q. Gan, X. Guan, W.-J. Huang, J.-C. Jiang, H. Li, Y.-P. Men, C. Sun, B.-J. Wang, H. G. Wang, S.-Q. Wang, J.-T. Xie, H. Xu, R. Yao, X.-P. You, D. J. Yu, J.-P. Yuan, R. Yuen, C.-F. Zhang, and Y. Zhu, *Research in Astronomy and Astrophysics* **21**, 107 (2021).

- D. J. Zhou, J. L. Han, J. Xu, C. Wang, P. F. Wang, T. Wang, W.-C. Jing, X. Chen, Y. Yan, W.-Q. Su, H.-Q. Gan, P. Jiang, J.-H. Sun, H.-G. Wang, N. Wang, S.-Q. Wang, R.-X. Xu, and X.-P. You, *Research in Astronomy and Astrophysics* **23**, 104001 (2023).
- J. L. Han, D. J. Zhou, C. Wang, W. Q. Su, Y. Yan, W. C. Jing, Z. L. Yang, P. F. Wang, T. Wang, J. Xu, N. N. Cai, J. H. Sun, Q. L. Yang, R. X. Xu, H. G. Wang, and X. P. You, *Research in Astronomy and Astrophysics* **25**, 014001 (2025).
- F. Jankowski, W. van Straten, E. F. Keane, M. Bailes, E. D. Barr, S. Johnston, and M. Kerr, *MNRAS* **473**, 4436 (2018).
- S. Sanidas, S. Cooper, C. G. Bassa, J. W. T. Hessels, V. I. Kondratiev, D. Michilli, B. W. Stappers, C. M. Tan, J. van Leeuwen, L. Cerrigone, R. A. Fallows, M. Iacobelli, E. Orrù, R. F. Pizzo, A. Shulevski, M. C. Toribio, S. ter Veen, P. Zucca, L. Bondonneau, J.-M. Grießmeier, A. Karastergiou, M. Kramer, and C. Sobey, *Astronomy & Astrophysics* **626**, A104 (2019).
- M. A. McLaughlin, A. G. Lyne, D. R. Lorimer, M. Kramer, A. J. Faulkner, R. N. Manchester, J. M. Cordes, F. Camilo, A. Possenti, I. H. Stairs, G. Hobbs, N. D'Amico, M. Burgay, and J. T. O'Brien, *nat* **439**, 817 (2006).
- D. J. McKenna, E. F. Keane, P. T. Gallagher, and J. McCauley, *MNRAS* **527**, 4397 (2024a).
- S. A. Tyul'bashev, V. S. Tyul'bashev, V. V. Oreshko, and S. V. Logvinenko, *Astronomy Reports* **60**, 220 (2016).
- S. A. Tyul'bashev, G. E. Tyul'basheva, M. A. Kitaeva, I. L. Ovchinnikov, V. V. Oreshko, and S. V. Logvinenko, *Monthly Notices of the Royal Astronomical Society* **528**, 2220 (2024).
- K. Stovall, R. S. Lynch, S. M. Ransom, A. M. Archibald, S. Banaszak, C. M. Biwer, J. Boyles, L. P. Dartez, D. Day, A. J. Ford, J. Flanigan, A. Garcia, J. W. T. Hessels, J. Hinojosa, F. A. Jenet, D. L. Kaplan, C. Karako-Argaman, V. M. Kaspi, V. I. Kondratiev, S. Leake, D. R. Lorimer, G. Lunsford, J. G. Martinez, A. Mata, M. A. McLaughlin, M. S. E. Roberts, M. D. Rohr, X. Siemens, I. H. Stairs, J. van Leeuwen, A. N. Walker, and B. L. Wells, *ApJ* **791**, 67 (2014).
- J. M. Cordes, P. C. C. Freire, D. R. Lorimer, F. Camilo, D. J. Champion, D. J. Nice, R. Ramachandran, J. W. T. Hessels, W. Vlemmings, J. van Leeuwen, S. M. Ransom, N. D. R. Bhat, Z. Arzumanyan, M. A. McLaughlin, V. M. Kaspi, L. Kasian, J. S. Deneva, B. Reid, S. Chatterjee, J. L. Han, D. C. Backer, I. H. Stairs, A. A. Deshpande, and C. A. Faucher-Giguère, *ApJ* **637**, 446 (2006).
- J. S. Deneva, K. Stovall, M. A. McLaughlin, S. D. Bates, P. C. C. Freire, J. G. Martinez, F. Jenet, and M. Bagchi, *ApJ* **775**, 51 (2013).
- C. Sobey, C. G. Bassa, S. P. O'Sullivan, J. R. Callingham, C. M. Tan, J. W. T. Hessels, V. I. Kondratiev, B. W. Stappers, C. Tiburzi, G. Heald, T. Shimwell, R. P. Breton, M. Kirwan, H. K. Vedantham, E. Carretti, J. M. Grießmeier, M. Haverkorn, and A. Karastergiou, *A&A* **661**, A87 (2022).
- S. Ransom, *Astrophysics Source Code Library*, ascl:1107.017 (2011).
- C. G. Bassa, Z. Pleunis, and J. W. T. Hessels, *Astronomy and Computing* **18**, 40 (2017).
- D. McKenna, E. Keane, P. Gallagher, and J. McCauley, *The Journal of Open Source Software* **9**, 5517 (2024b).
- P. C. Murphy, Callanan, P., McCauley, J., McKenna, D. J., Fionnagáin, D. Ó, Louis, C. K., Redman, M. P., Cañizares, L. A., Carley, E. P., Maloney, S. A., Coghlan, B., Daly, M., Scully, J., Dooley, J., Gajjar, V., Giese, C., Brennan, A., Keane, E. F., Maguire, C. A., Quinn, J., Mooney, S., Ryan, A. M., Walsh, J., Jackman, C. M., Golden, A., Ray, T. P., Doyle, J. G., Rigney, J., Burton, M., and Gallagher, P. T., *A&A* **655**, A16 (2021).
- W. van Straten and M. Bailes, *Publications of the Astronomical Society of Australia* **28**, 1 (2011).
- Y. Collet and M. Kucherawy, *Zstandard Compression and the application/zstd Media Type*, Tech. Rep. RFC 8478 (Internet Engineering Task Force, 2018).
- A. W. Hotan, W. van Straten, and R. N. Manchester, *Publications of the Astronomical Society of Australia* **21**, 302 (2004).
- V. Morello, E. D. Barr, S. Cooper, M. Bailes, S. Bates, N. D. R. Bhat, M. Burgay, S. Burke-Spolaor, A. D. Cameron, D. J. Champion, R. P. Eatough, C. M. L. Flynn, A. Jameson, S. Johnston, M. J. Keith, E. F. Keane, M. Kramer, L. Levin, C. Ng, E. Petroff, A. Possenti, B. W. Stappers, W. van Straten, and C. Tiburzi, *Monthly Notices of the Royal Astronomical Society* **483**, 3673 (2019).
- G. B. Hobbs, R. T. Edwards, and R. N. Manchester, *Monthly Notices of the Royal Astronomical Society* **369**, 655 (2006).
- V. I. Kondratiev, J. P. W. Verbiest, J. W. T. Hessels, A. V. Bilous, B. W. Stappers, M. Kramer, E. F. Keane, A. Noutsos, S. Osłowski, R. P. Breton, T. E. Hassall, A. Alexov, S. Cooper, H. Falcke, J.-M. Grießmeier, A. Karastergiou, M. Kuniyoshi, M. Pilia, C. Sobey, S. ter Veen, J. van Leeuwen, P. Weltevrede, M. E. Bell, J. W. Broderick, S. Corbel, J. Eislöffel, S. Markoff, A. Rowlinson, J. D. Swinbank, R. a. M. J. Wijers, R. Wijnands, and P. Zarka, *Astronomy & Astrophysics* **585**, A128 (2016).
- J. Dowell, G. B. Taylor, F. K. Schinzel, N. E. Kassim, and K. Stovall, *MNRAS* **469**, 4537 (2017).
- D. C. Price, *Research Notes of the AAS* **5**, 246 (2021).
- S. J. Wijnholds and W. A. van Cappellen, *IEEE Transactions on Antennas and Propagation* **59**, 1981 (2011).
- T. Carozzi, "dreamBeam." (2020).
- M. Newville, R. Otten, A. Nelson, A. Ingargiola, T. Stensitzki, D. Allan, A. Fox, F. Carter, Michal, R. Osborn, D. Pustakhod, Ineuhaus, S. Weigand, Glenn, C. Deil, Mark, A. L. R. Hansen, G. Pasquevich, L. Foks, N. Zobrist, O. Frost, A. Beelen, Stuermer, azelcer, A. Hannum, A. Polloreno, J. H. Nielsen, S. Caldwell, A. Almarza, and A. Persaud, "Lmfit/lmfit-py: 1.0.3." Zenodo (2021).
- A. V. Bilous, V. I. Kondratiev, M. Kramer, E. F. Keane, J. W. T. Hessels, B. W. Stappers, V. M. Malofeev, C. Sobey, R. P. Breton, S. Cooper, H. Falcke, A. Karastergiou, D. Michilli, S. Osłowski, S. Sanidas, S. ter Veen, J. van Leeuwen, J. P. W. Verbiest, P. Weltevrede, P. Zarka, J. M. Grießmeier, M. Serylak, M. E. Bell, J. W. Broderick, J. Eislöffel, S. Markoff, and A. Rowlinson, *A&A* **591**, A134 (2016).
- S. A. Tyul'bashev, V. S. Tyul'bashev, and V. M. Malofeev, *Astronomy and Astrophysics* **618**, A70 (2018).
- A. Seymour, D. Michilli, and Z. Pleunis, *Astrophysics Source Code Library*, ascl:1910.004 (2019), aDS Bibcode: 2019ascl.soft10004S.
- CHIME/FRB Collaboration, B. C. Andersen, K. Bandura, M. Bhardwaj, P. Boubel, M. M. Boyle, P. J. Boyle, C. Brar, T. Cassanelli, P. Chawla, D. Cubranic, M. Deng, M. Dobbs, M. Fandino, E. Fonseca, B. M. Gaensler, A. J. Gilbert, U. Giri, D. C. Good, M. Halpern, A. S. Hill, G. Hinshaw, C. Höfer, A. Josephy, V. M. Kaspi, R. Kothes, T. L. Landecker, D. A. Lang, D. Z. Li, H. H. Lin, K. W. Masui, J. Mena-Parra, M. Merryfield, R. Mckinven, D. Michilli, N. Milutinovic, A. Naidu, L. B. Newburgh, C. Ng, C. Patel, U. Pen, T. Pihonneault-Marotte, Z. Pleunis, M. Rafei-Ravandi, M. Rahman, S. M. Ransom, A. Renard, P. Scholz, S. R. Siegel, S. Singh, K. M. Smith, I. H. Stairs, S. P. Tendulkar, I. Tret'yakov, K. Vanderlinde, P. Yadav, and A. V. Zwaniga, *ApJ* **885**, L24 (2019).
- S. K. Ocker and J. M. Cordes, *The Astrophysical Journal* **1002**, 3 (2026).
- M. Pitkin, *Journal of Open Source Software* **3**, 538 (2018).
- F. A. Dong, K. Crowter, B. W. Meyers, Z. Pleunis, I. Stairs, C. M. Tan, T. T. Yu, P. J. Boyle, A. M. Cook, E. Fonseca, B. M. Gaensler, D. C. Good, V. Kaspi, J. W. McKee, C. Patel, and A. B. Pearlman, *MNRAS* **524**, 5132 (2023).
- E. v. d. Wateren, C. G. Bassa, S. Cooper, J.-M. Grießmeier, B. W. Stappers, J. W. T. Hessels, V. I. Kondratiev, D. Michilli, C. M. Tan, C. Tiburzi, P. Weltevrede, A.-S. B. Nielsen, T. D. Carozzi, B. Ciardi, I. Cognard, R.-J. Dettmar, A. Karastergiou, M. Kramer, J. Künsemöller, S. Osłowski, M. Serylak, C. Vocks, and O. Wucknitz, *Astronomy & Astrophysics* **669**, A160 (2023).
- E. Parent, H. Sewalls, P. C. C. Freire, T. Matheny, A. G. Lyne, B. B. P. Perera, F. Cardoso, M. A. McLaughlin, B. Allen, A. Brazier, F. Camilo, S. Chatterjee, J. M. Cordes, F. Crawford, J. S. Deneva, F. A. Dong, R. D. Ferdman, E. Fonseca, J. W. T. Hessels, V. M. Kaspi, B. Knispel, J. v. Leeuwen, R. S. Lynch, B. M. Meyers, J. W. McKee, M. B. Mickaliger, C. Patel, S. M. Ransom, A. Rochon, P. Scholz, I. H. Stairs, B. W. Stappers, C. M. Tan, and W. W. Zhu, *The Astrophysical Journal* **924**, 135 (2022).
- W. Fiore, L. Levin, M. A. McLaughlin, A. Anumarlapudi, D. L. Kaplan, J. K. Swiggum, G. Y. Agazie, R. Bavisotto, P. Chawla, M. E. DeCesar, T. Dolch, E. Fonseca, V. M. Kaspi, Z. Komassa, V. I. Kondratiev, J. van Leeuwen, E. F. Lewis, R. S. Lynch, A. E. McEwen, R. Mundorf, H. Al Noori, E. Parent, Z. Pleunis, S. M. Ransom, X. Siemens, R. Spiewak, I. H. Stairs, M. Surnis, and T. J. Tobin, *ApJ* **956**, 40 (2023).
- T. E. E. Olszanski, E. F. Lewis, J. S. Deneva, M. A. McLaughlin, K. Stovall, P. C. C. Freire, B. B. P. Perera, M. Bagchi, and J. G. Martinez, *arXiv e-prints*, arXiv:2502.04571 (2025).

Source	Detected Sources				
	Cat.	N _{obs}	N _{det}	T _{obs} (h)	T _{max} (min)
J0104+6438	GL	39	34	20.4	153
J0146+3055	P	23	22	24.6	149
J0220+3626	PL	22	21	19.1	120
J0226+3356	C	16	15	26.0	178
J0317+1328	LP	17	10	12.6	154
J0350+2341	P	1	1	1.0	59
J0355+2838	GL	33	29	28.6	89
J0608+1635	AL	42	40	18.3	59
J0928+3037	P	1	1	1.0	59
J1110+58	G	1	1	1.0	59
J1132+2514	LP	33	31	23.7	89
J1239+32	G	2	2	2.0	59
J1243+3946	LP	26	25	19.8	104
J1327+3423	GLP	15	15	6.1	59
J1536+1749	P	33	18	47.7	179
J1832+2749	AL	40	38	34.2	120
J1836+5156	GL	41	36	32.9	149
J1844+21	P	1	1	1.0	59
J1958+2213	P	1	1	1.0	59
J2000+2920	GL	36	34	38.4	119
J2105+1908	P	15	7	17.6	119
J2202+2134	P	36	34	28.5	134
J2347+0300	AL	24	22	18.1	119

TABLE 4

SOURCES OBSERVED FOR THIS WORK, WITH A DISTINCTION BETWEEN DETECTED AND NON-DETECTED SOURCES AT THE IRISH LOFAR STATION. THE COLUMNS CONTAIN THE NUMBER OF OBSERVATIONS, THE NUMBER OF DETECTIONS, THE TOTAL OBSERVING TIME ON THE SOURCE AND THE LONGEST SINGLE POINTING ON THE SOURCE. FOR CATALOGUES, “A” REPRESENTS SURVEYS CONDUCTED WITH THE Arecibo telescope, “G” IS THE GBNCC SURVEY, “L” IS THE LOTAAS SURVEY, AND “P” ARE THE PRAO CATALOGUES.

A. E. McEwen, J. K. Swiggum, D. L. Kaplan, C. M. Tan, B. W. Meyers, E. Fonseca, G. Y. Agazie, P. Chawla, K. Crowter, M. E. DeCesar, T. Dolch, F. A. Dong, W. Fiore, E. Fonseca, D. C. Good, A. G. Istrate, V. M. Kaspi, V. I. Kondratiev, J. van Leeuwen, L. Levin, E. F. Lewis, R. S. Lynch, K. W. Masui, J. W. McKee, M. A. McLaughlin, H. Al Noori, E. Parent, S. M. Ransom, X. Siemens, R. Spiewak, and I. H. Stairs, *ApJ* **962**, 167 (2024).

D. Teplikh, V. Malofeev, O. Malov, and S. Tyul’bashev, *Open Astronomy* **31**, 166 (2022).

A. E. McEwen, R. Spiewak, J. K. Swiggum, D. L. Kaplan, W. Fiore, G. Y. Agazie, H. Blumer, P. Chawla, M. DeCesar, V. M. Kaspi, V. I. Kondratiev, M. LaRose, L. Levin, R. S. Lynch, M. McLaughlin, M. Mingyar, H. A. Noori, S. M. Ransom, M. S. E. Roberts, A. Schmiedekamp, C. Schmiedekamp, X. Siemens, I. Stairs, K. Stovall, M. Surnis, and J. v. Leeuwen, *The Astrophysical Journal* **892**, 76 (2020).

S. A. Tyul’bashev, G. E. Tyul’basheva, and M. A. Kitaeva, in *Proceedings of The Multifaceted Universe: Theory and Observations - 2022 — PoS(MUTO2022)*, Vol. 425 (SISSA Medialab, 2022) p. 043.

D. McKenna, “Data produced as a part of a pulsar timing campaign with the irish lofar station between 2020 and 2023 at 150 mhz,” (2025a).

D. McKenna, “Pulsar timing ephemerides produced as a part of an observing campaign with the irish lofar station between 2020 and 2023 at 150 mhz,” (2025b)

APPENDIX

OBSERVED SOURCES

Table 4 contains a list of the sources observed as a part of this work if they were detected, while Table 5 contains sources that were not detected. Each source lists the number of times they were observed and detected, alongside the total time spent observing each source, and the minimum and maximum time spent observing the source in one observation.

PULSAR PROFILES

Figure 2 contains the 1-dimensional, folded, dedispersed and time-scrunched profiles for the 17 pulsars monitored as a part of this work.

This paper was built using the Open Journal of Astrophysics L^AT_EX template. The OJA is a journal which provides fast and easy peer review for new papers in the **astro-ph** section of the arXiv, making the reviewing process simpler for authors and referees alike. Learn more at <http://astro.theoj.org>.

Source	Non-detected Sources				
	Cat.	N _{obs}	N _{det}	T _{obs} (h)	T _{max} (min)
J0109+11	P	2	0	2.0	59
J0305+1127	P	2	0	3.7	164
J0357-05	G	1	0	1.0	61
J0509+37	P	2	0	3.0	119
J0933+3245	P	1	0	1.0	59
J1243+1752	P	3	0	3.3	78
J1354+24	G	6	0	5.4	59
J1430+22	G	5	0	5.2	109
J1439+76	G	7	0	6.4	85
J1651+1422	P	3	0	4.9	119
J1843+21	P	2	0	2.9	114
J1844+4117	P	1	0	1.0	59
J1921+34	P	1	0	1.0	62
J2029+34	P	1	0	1.2	74
J2253+1237	P	2	0	2.7	104
J2333+20	P	1	0	1.0	59

TABLE 5

SOURCES OBSERVED FOR THIS WORK, BUT WERE NOT DETECTED. COLUMNS AND CATALOGUE LEGEND MATCHES THE INFORMATION PROVIDED IN TABLE 4

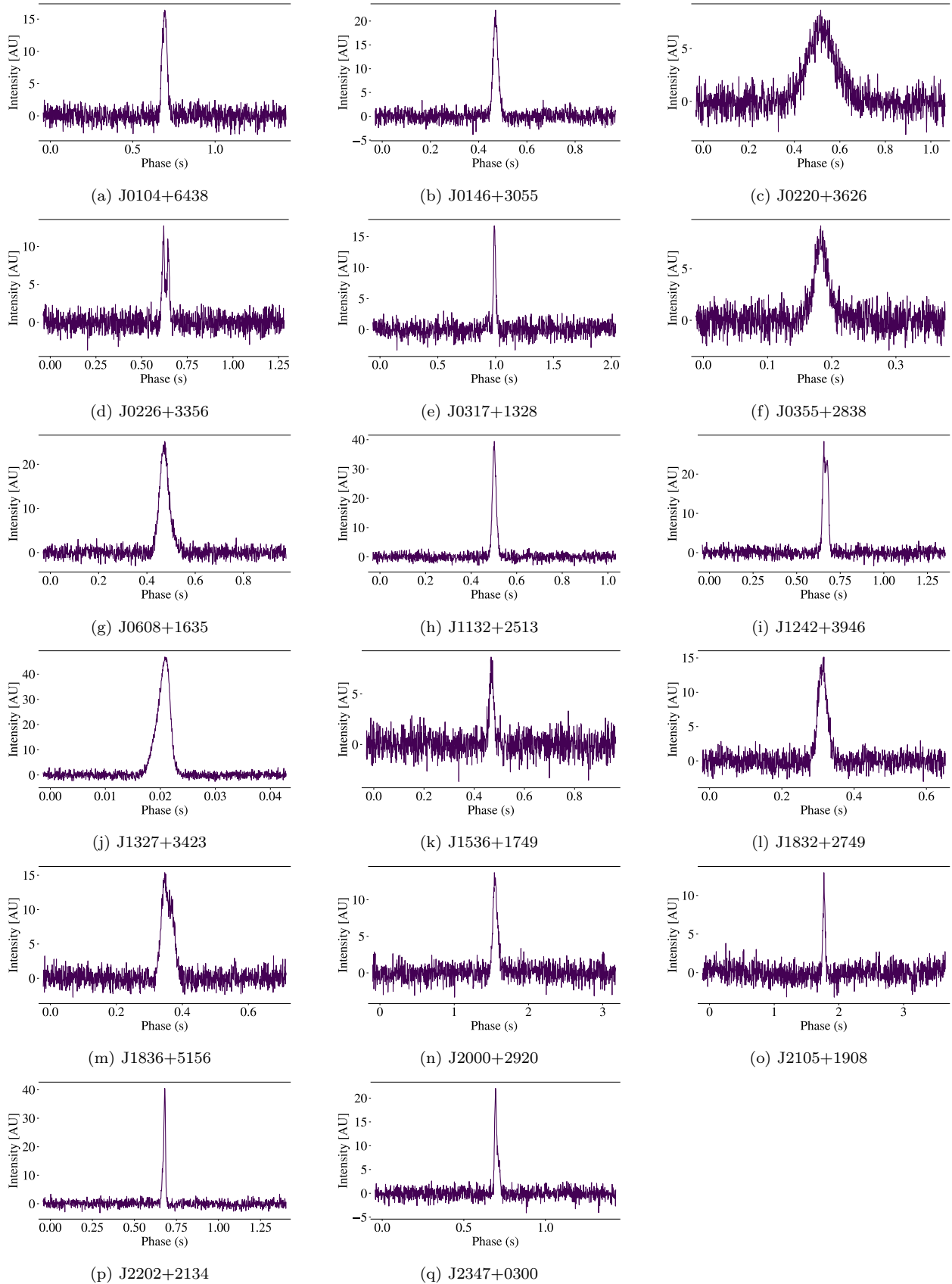


FIG. 2.— The Stokes I frequency-averaged folded profiles of the sources detected and monitored as a part of this work. The x-axis labels cover the full folded pulse profile of each source in seconds, while the y-axis contains off-axis-normalised emission in arbitrary units.